The coupling between atomic and electronic structure in small Cu clusters

1993 J. Phys.: Condens. Matter 5 5591

(http://iopscience.iop.org/0953-8984/5/31/021)

J. Phys.: Condens. Matter 5 (1993) 5591–5602. Printed in the UK

The coupling between atomic and electronic structure in small Cu clusters

O B Christensen† and K W Jacobsen‡

† Nordita, Blegdamsvej 17, DK-2100 København Ø, Denmark

‡ Laboratory of Applied Physics, Technical University of Denmark, DK-2800 Lyngby, Denmark

Received 20 April 1993

Abstract. Thermodynamic and ground-state properties of Cu clusters have been studied with the effective-medium theory including a tight-binding description of the one-electron spectrum. Simulated-annealing Monte Carlo calculations have been performed for cluster sizes between 3 and 29 to determine ground-state energies and structures. Finite-temperature ensembles have been generated for a range of temperatures. The magic numbers 8, 18 and 20 are reproduced and remain stable at temperatures close to 1000 K, where the clusters may be regarded as liquid. The coupling between the atomic and electronic degrees of freedom through a Jahn–Teller-like effect is shown to play a key role in understanding the stability of the magic clusters at high temperatures. For the non-magic clusters this Jahn–Teller effect gives rise to large Fermi gaps even at high temperatures and a pronounced stability of the even-sized clusters relative to those with odd sizes. Finite-temperature electronic spectra are calculated. The fluctuations in the atomic positions give rise to a large broadening of the electronic levels, in agreement with experimental observations. Cu_{13} exhibits a rather sharp melting transition, whereas clusters of other sizes show more complex behaviour.

1. Introduction

The physics of metal clusters is a field that has developed rapidly over the last few years [1]. Clusters of certain sizes (magic numbers) exhibit an extraordinary stability [1], in much the same way as is the case with nuclei. Magic numbers are seen in abundance measurements, ionization potentials, dissociation energies etc. They were first observed for Na [2], but the same magic numbers have also been seen for other monovalent free-electron-like metals. Katakuse and co-workers [3] performed abundance measurements for positively charged clusters of Cu, Ag and Au.

The magic numbers correspond to closed angular momentum shells, and this idea has been illustrated in a number of simple models with the common characteristic that the ion cores have only been taken into account in a very approximate way. Clemenger [4] applied the Nilsson model [5] of nuclear physics to metallic clusters. Here, the one-electron levels are constructed as eigenvalues of a simple spheroidal harmonic oscillator. In a study by Ekardt [6] the ion cores were replaced by a homogeneous positively charged sphere. Local-density calculations on the system of valence electrons reproduced the magic numbers observed for Na. In this model the geometry of the cluster was initially ignored. Later, spatial structure was introduced through a spheroidal distortion of the jellium spheres [7].

Calculations including the atomic cores have been performed at different levels of approximation. Cluster sizes larger than 13 have been treated almost entirely by very simple

0953-8984/93/315591+12$07.50

models. An extensive calculation with the simple Hückel model [8] has been performed by Lindsay and co-workers. Small clusters have been treated in configuration–interaction calculations; for instance, the relaxed ground-state of Na-clusters of up to eight atoms have been determined [9]. Local-density calculations including the ion-cores have been done mainly for the ground state of small alkali clusters consisting of a maximum of 13 atoms [10, 11]. Andreoni and co-workers [12] also performed calculations for Na_{18} and Na_{20} with the Car–Parrinello method, where the ground state was found with simulated annealing and where finite-temperature properties were investigated.

The experimental knowledge of the atomic structure of clusters is very sparse. Only the structures of some clusters up to seven atoms have been determined [13].

In the present work we have applied a model for the binding in a metal cluster, which includes a description of the atomic degrees of freedom but which is still computationally sufficiently simple to allow for studies of many cluster sizes over a wide temperature range. In the following section we will describe the model, the effective-medium theory [14] including a tight-binding description of the one-electron spectrum. In the third section we describe and discuss the results of applying the model to small Cu clusters. We shall discuss the interplay between 'magicity' and geometry, and show that atomic relaxations are very important in understanding the extraordinary stability of clusters with magic sizes. Sizeable Fermi gaps also exist in non-magic clusters with an even number of atoms. The influence of heating of the atomic degrees of freedom on stability is treated, and the effect of high temperatures on the electronic spectrum is discussed. The melting of small clusters is also studied. It is shown that Cu_{13} has a well defined melting transition at $T \simeq 450\,\mathrm{K}$. Other cluster sizes exhibit a more complex behaviour.

A brief account of some of the results discussed here has been presented in [15].

2. The effective-medium model

To study the coupling between the atomic and electronic degrees of freedom in small Cu clusters we construct a model which can be used to calculate the total energy and the electronic structure of a cluster as a function of atomic positions. The method applied in the present work is the effective-medium theory (EMT) [14]. It has the property of reproducing a well tested interatomic potential for an infinite system of metallic Cu and it takes finite-size shell effects into account through a tight-binding description. The effective-medium model is based on density functional theory and relies on the fact that errors in the total electron density give rise to only second-order errors in the total energy due to the variational properties of the energy functional. The idea behind the EMT is to approximate the energetics of an atom in a metallic environment by a simple reference system, which can be taken as the atom embedded in a homogeneous electron gas or as the atom situated in a perfect FCC crystal with a suitable lattice constant. In the following presentation we shall use the FCC crystal as the reference system. The EMT total-energy expression may be written as

$$E_{\mathrm{tot}} = \sum_{\text{atoms } i} E_{\mathrm{c}}(\bar{n}_i) + \sum_{\text{atoms } i} E_{\mathrm{AS}}^{(i)} + E_{\mathrm{I-el}} \tag{1}$$

as described in detail elsewhere [14]. The cohesive energy function E_{c} describes the energy of an FCC crystal of a lattice constant corresponding to a background electron density of $\bar{n}$ felt by each atom. The atomic-sphere correction energy E_{AS} represents the repulsion between overlapping atomic spheres and plays an important role in non-close-packed structures where

the overlap is significant. The one-electron correction E_{1-el} is a correction concerning the difference in density of states (DOS) between the reference system and the real system.

For a finite system like a cluster of Cu atoms the electron DOS consists of a discrete set of levels which are not well represented by the DOS of an infinite FCC Cu crystal. It is therefore necessary to include the one-electron energy in the description of the energetics of small clusters. The one-electron energy E_{1-el} is the energy difference due to the formation of electronic shells instead of a continuum as in the extended FCC system, and we shall therefore in the following use the term *shell energy* to be synonymous with the one-electron energy.

The important shell structure in small Cu clusters is due to the 4s electrons. The centre of the 4p band of bulk Cu is situated approximately one Rydberg above the centre of the 4s band [16], and we shall therefore ignore atomic p orbitals in our description. We shall also ignore the filled 3d orbitals. In a more accurate description the p and d orbitals could be included; but since the one-electron energy is only a small correction term which describes deviations in the electronic structure from that in an FCC crystal, a simple model of the s band is sufficient.

The bonding between the atomic s orbitals is described with a tight-binding Hamiltonian. We assume for simplicity that all the atomic s levels are at the same energy and choose our energy zero at this common energy. We determine the distance dependence of the off-diagonal matrix elements H_{ij} between atomic s orbitals situated at atoms i and j in the following way. The matrix elements can be expected to decay in the same way as an orbital on one of the atoms, which again falls off roughly as the square root of the electron density. In the construction of the embedding densities an exponential fall-off is used:

$$\bar{n}_i \propto \sum_{j \neq i} \mathrm{e}^{-\eta_2 r_{ij}} \tag{2}$$

where η_2 is a parameter characteristic of Cu†. We therefore take the hopping matrix elements to be of the form

$$H_{ij} = -V_0 \, \mathrm{e}^{-(\eta_2/2)(r_{ij}-r_0)} \qquad i \neq j \tag{3}$$

where r_0 is the equilibrium nearest-neighbour distance between Cu atoms in an FCC crystal. The prefactor V_0 is determined so that the width of the occupied part of the s band in the tight-binding model for an FCC crystal at equilibrium volume agrees with the one calculated self-consistently by Moruzzi and co-workers [17]. The value obtained in this way is $V_0 = 0.567\,\mathrm{eV}$.

For a given atomic configuration of a cluster the tight-binding Hamiltonian is used to calculate the discrete electron spectrum with energies ϵ_α of the cluster. The band energy $E_{\mathrm{band}}^{\mathrm{FCC}}$ in the reference FCC system should be subtracted in the one-electron energy correction. The band energy is a function of the embedding density $\bar{n}$, and this function can be calculated once and for all by solving the tight-binding Hamiltonian for a range of lattice constants of an FCC lattice. The shell energy therefore takes the form

$$E_{1-el} = \sum_{\text{occupied}} \epsilon_\alpha - \sum_i E_{\mathrm{band}}^{\mathrm{FCC}}(\bar{n}_i). \tag{4}$$

To summarize, we have described an effective-medium model for the total energy of a cluster as a function of atomic positions. The model consists of energy terms which describe the local volume changes through embedding densities, electrostatic interactions by use of pair potentials, and the shell energy by a tight-binding Hamiltonian.

† A table with all the effective-medium parameters for Cu can be found in [14].

3. Results and discussion

We have performed a number of simulated-annealing Monte Carlo calculations with the Metropolis algorithm [18] to determine the ground-state configurations of small Cu clusters. The simulations have been done both with and without the inclusion of the shell energy E_{1-el}. Typically 2–5 runs of 2000 coordinate sweeps were made at a given cluster size, starting at temperatures in the range 2000–10 000 K. A sweep involves one trial movement of each coordinate, i.e. $3N$ total-energy calculations. Finite-temperature ensembles were generated using 10 000–40 000 sweeps.

3.1. Ground-state properties

In this section we present and discuss the calculated ground-state properties of the clusters. First, we present the obtained ground-state energies and atomic structures and compare them with results from other models and experiment in the cases where it is possible. We then discuss the coupling between the electronic and atomic structure via the Jahn–Teller effect. This coupling is crucial in understanding the extraordinary stability of the magic clusters and the pronounced even–odd oscillations observed in experimental abundance spectra [3].

The calculated ground-state energies are depicted in figure 1. We measure E_c from the minimum value, which is 3.56 eV below the atomic energy. Through the points a smooth three-parameter curve is drawn with the form

$$E_{fit} = aN + bN^{2/3} + cN^{1/3} \tag{5}$$

where the first term represents a bulk energy per atom, the second represents a surface energy term and the third a curvature term. The magic cluster sizes show up as tiny oscillations on the curve. As a convenient way of extracting the magic numbers we plot in figure 2 the deviation of the total energies from the fit (5).

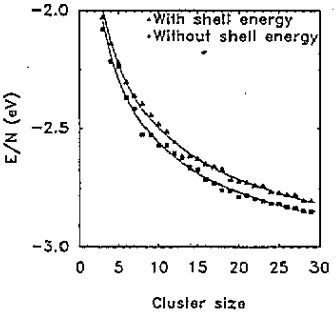

Figure 1. Total energy as a function of cluster size. The triangles are obtained with a full calculation while the squares result from a calculation where the shell energy E_{1-el} is neglected. The curves are fits to the data with the analytic form of (5).

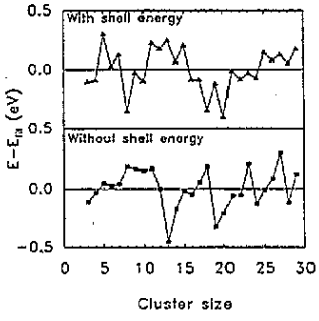

Figure 2. Deviation of total energy from the fit (5). The triangles are obtained with a full calculation while the squares result from a calculation where the shell energy E_{1-el} is neglected.

A different way of enhancing the fine structure is to take the second difference

$$\Delta_2(N) = E(N+1) + E(N-1) - 2E(N). \tag{6}$$

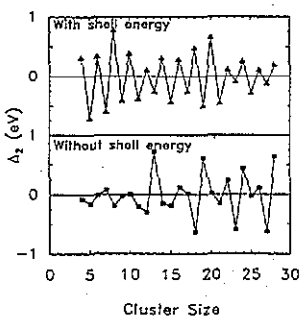

Figure 3. Second difference of the total energy, $E(N+1) + E(N-1) - 2E(N)$. The triangles are obtained with a full calculation while the squares result from a calculation where the shell energy E_{1-el} is neglected.

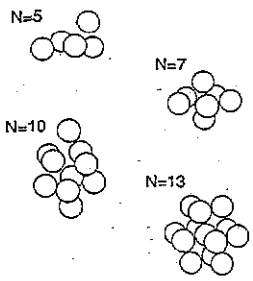

Figure 4. Calculated ground-state structures for $N = 5$, 7, 10 and 13.

This quantity is shown in figure 3. Assuming thermal equilibrium it follows [1] that the value of $\Delta_2(N)$ is proportional to the logarithm of the abundance of N clusters in an experimental beam.

It is clear from the figures that the clusters of size 8, 18 and 20 are particularly stable. This means that the tight-binding form used to model the shell energy is indeed able to reproduce the magic numbers seen in experiment [2, 3] and in other models [2, 4, 6]. The magic numbers do not appear in the calculations where the shell energy is neglected. Without the shell energy the ground-state configurations are close-packed and the sizes 13 and 19 appear as magic corresponding to close-packed ground-state structures with a central atom surrounded by all atoms up to first and second nearest-neighbour shells, respectively.

The s-state tight-binding model for calculating the shell energy is general for monovalent metals, and the ground-state structures found in the present calculation are in fact very similar to previously published theoretical [8–10, 19] and experimental [13] results for alkali clusters. For instance, in the case of $N = 7$ the equilibrium structure is a fivefold bi-pyramid (see figure 4) as indicated by electron spin resonance experiments on Li [13]. For $N = 13$ we find a cuboctahedral rather than an icosahedral geometry like the Na result of [10]. Structures for cluster sizes $N = 5$, 7, 10 and 13 are shown in figure 4. In figure 5 we compare the structure for the $N = 20$ Cu cluster with the structure for Na_{20} found with the Car–Parrinello method [12] by Ballone and co-workers. The two structures are very similar, indicating that the cluster structures for the two different metals are determined by the same mechanisms.

To study the variation of the shape of the clusters as a function of size we have evaluated the eccentricities. We define the eccentricity of a cluster as follows. The inertial (3×3) matrix is defined as usual as

$$\overline{\overline{J}}_{ij} = \sum_k [|r_k - \bar{r}|^2 \delta_{ij} - (r_k - \bar{r})_i (r_k - \bar{r})_j] \tag{7}$$

where $i, j = 1, 2, 3$ are the coordinates and $\bar{r} = (1/N) \sum_k r_k$ is the centre of mass of the cluster. The three eigenvalues J_i of this matrix are the moments of inertia. In the case of an ellipsoid of axes a_i, these are also principal inertial axes with $J_i \propto a_i^2$. Thus we define the two eccentricities of a cluster as

$$\epsilon_{1,2} = \sqrt{J_{1,2}/J_3} \qquad J_1 \leqslant J_2 \leqslant J_3. \tag{8}$$

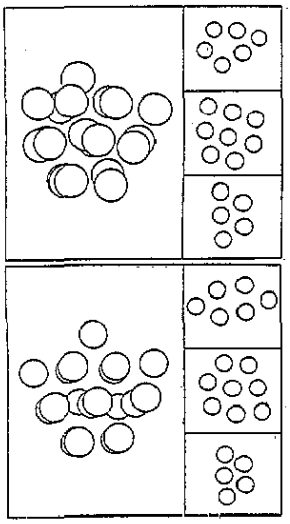

Figure 5. Ground-state structure for $N = 20$ from our calculation (top panel) and from the local-density calculation of [12] for a Na_{20} cluster (bottom panel).

In figure 6 we plot the two calculated eccentricities for the ground-state structures. For comparison we also show eccentricities determined from a calculation by Selby and co-workers [20]. In the latter calculation the principal axes are related to vibrational frequencies of a three-dimensional harmonic oscillator potential, and the energy is minimized with respect to one distortion parameter. This so-called Nilsson model [5] was first applied to metallic clusters by Clemenger [4].

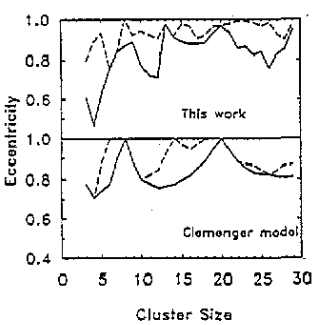

Figure 6. Eccentricities of ground-state structures from the present model (top panel) and from the Clemenger model [24] (bottom panel).

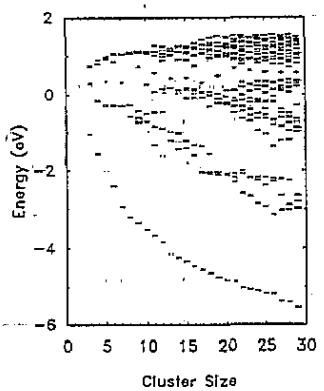

Figure 7. One-electron levels in the calculated cluster ground-state configurations. The highest occupied levels are indicated by dots (one for each electron on the level).

As predicted by the Clemenger model, the magic clusters prefer a spherical geometry, whereas non-magic clusters tend to be distorted. One feature present in our calculation, but not in the Clemenger model, is the almost spherical geometry of $N = 13$. The minimization of the electrostatic repulsion of the ionic nuclei leads to a close-packed cuboctahedral structure of the 13 cluster. This fact was already established in local-density calculations by Martins and co-workers [10]. The observation that the tendency to close-packing may

be important for determining the ground-state structure, at the same time as the total energy has a size-dependence corresponding to angular momentum level bunchings, has been established experimentally for larger Cu clusters [21].

We now turn to a more detailed discussion of the electronic structure which results from the present model and the interplay with the atomic arrangement.

The tight-binding Hamiltonian (3) has only N eigenvalues and it is therefore clearly unable to reproduce the full infinite spectrum of angular momentum levels. However, as has been shown for instance in the framework of the LMTO method [16] a tight-binding description may give a good representation of the electronic structure in a certain energy window. In figure 7 we plot the one-electron spectrum of the equilibrium structure as a function of cluster size. The lower levels bunch up in a lowest band of one state and a second-lowest of three states, thus reproducing one s and three p states. For the largest clusters a d band of five states is recognized. The grouping of levels in s, p and d shells is also seen in the spectra calculated by Lindsay and co-workers [8] for the ground states of simple Hückel clusters. In both calculations, though, the similarity to an angular momentum spectrum is only valid some levels below the Fermi level at $N/2$.

At all even cluster sizes, the ground state has a noticeable Fermi gap irrespective of whether there should be a shell closing or not according to the angular momentum model. This is illustrated in figure 8. The gap is largest at the magic numbers, but is quite large at all sizes. Also shown in figure 8 are experimentally observed gaps for Cu_N^- determined with photoelectron spectroscopy [22]. We see that the calculated gaps are in fair agreement with the experimentally determined values both with regard to the absolute size and the trend when the size of the cluster is changed. Note in particular that the ratio between a typical gap for a magic and a non-magic cluster is well reproduced. This ratio is clearly exaggerated in simpler models where the atomic degrees of freedom are neglected [22]. Oscillations in the cluster energy are seen in experiment [1, 3], but are *not* of any appreciable size in the jellium-ball model of Ekardt [6] or the Clemenger model [4] compared with the strength of the magic numbers. One should bear in mind that the experimentally measured gap applies to geometries assumed by negatively charged clusters and is therefore different from the gap we calculate for the ground state of the neutral species—it does, however, give an estimate of the relevant order of magnitude of the quantities considered.

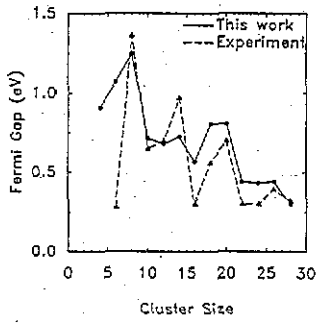

Figure 8. Calculated Fermi gaps in the cluster ground states (circles/full curve) compared with experimentally [22] determined gaps for Cu_N^- (triangles/broken curve).

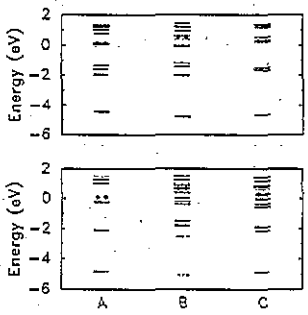

Figure 9. One-electron spectrum for three different atomic structures for $N = 16$ (top panel) and $N = 20$ (bottom panel). (A) Ground-state structure. (B) Continuum structure where the shell energy has been neglected. (C) FCC structure. The Fermi gap is much smaller in the two latter structures.

The existence of Fermi gaps for the non-magic clusters and the observation of an even–odd oscillation of the ground-state energy as a function of cluster size lead to the conjecture that a Jahn–Teller-like effect is decisive in determining the ground-state structures [23]. In the case of an even-sized cluster a small distortion can give rise to the opening of a gap between the occupied and the unoccupied levels with a gain in the total energy as a result.

To confirm that the Jahn–Teller effect is responsible for the even–odd oscillation, we have calculated the electronic spectra and the total energies of clusters in two alternative sets of atomic structures. The first of these, which we shall call the continuum structures, are the ground-state structures for the energy expression (1) without the shell energy E_{1-el}. These structures represent ground-state structures if the interatomic interactions are like in the bulk metallic system where the electronic spectrum is continuous. The second set of structures are simply pieces of an FCC crystal which are chosen to be as spherical as possible. This set we call the FCC structures. The lattice constant for the FCC structures are chosen to minimize the full energy expression (1). In figure 9 we show one-electron levels for clusters of size $N = 16$ and $N = 20$ in the three different structures: the ground-state structure, the continuum structure, and the FCC structure. It is clear that the gap is much smaller for the latter two atomic structures. Also, if we consider the total energy evaluated with the full expression (1) versus cluster size for the continuum or FCC structures (figure 10) we see no special stability of the magic sizes 8, 18 and 20. This lack of extra stability at the magic sizes is not due to the overall shape of the clusters because the continuum and FCC structures are just as spherical as the ground-state structures. This is therefore a strong indication that the relaxation of the atomic structure is of crucial importance in explaining the stability of the magic clusters. The atomic and electronic structure must therefore be treated simultaneously as in the present model so the atomic positions are allowed to relax to minimize the total energy including the shell energy.

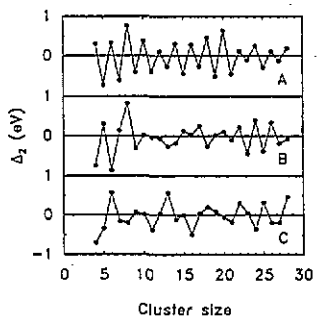

Figure 10. Second energy difference evaluated using (1). The three structures are (A) the ground-state structures, (B) the continuum structures found by neglecting the shell energy, and (C) a maximally spherical section of an FCC lattice. Only the sequence of fully relaxed ground-state structures show the magic numbers 8, 18 and 20. The even–odd fluctuation of the energy is also absent in the two lower curves.

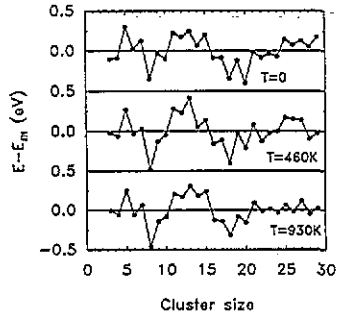

Figure 11. Energy deviation from the fit (5). Top panel: $T = 0$. Middle panel: $T = 460$ K. Bottom panel: $T = 930$ K. The magic numbers 8, 18 and 20 remain stable.

In summary, we have seen that the effective-medium model reproduces many qualitative ground-state features of simpler jellium and Hückel models and also agrees with more firmly based first-principles calculations and experimental results where available. The model

indicates that the coupling between the atomic and electronic structures via relaxations is of importance in explaining the extraordinary stability of large clusters at the magic numbers and also in understanding the electronic spectra, which also exhibit sizable Fermi gaps for clusters of (even) non-magic sizes, as observed with photoelectron spectroscopy [22].

3.2. Finite-temperature properties

In this section we discuss some aspects of the behaviour of small Cu clusters at high temperatures. We shall show that the extraordinary stability of the magic clusters survive even in a temperature regime where the clusters can be regarded as melted. We also discuss the electronic spectrum at elevated temperatures. Due to the coupling of the electronic structure to the atomic degrees of freedom the spectral peaks are broadened considerably. The peak widths are proportional to $\sqrt{T}$.

In figure 11 we plot the deviation from the fit (5) (as in figure 2) for Monte Carlo generated ensembles at $T = 460\,\mathrm{K}$ and $T = 930\,\mathrm{K}$. The energy variation at $T = 460\,\mathrm{K}$ is almost identical to that in the ground state, and even though the minimum at $N = 20$ is somewhat weaker at $T = 930\,\mathrm{K}$ than at $T = 0$, the spectra are very similar. The magic numbers 8, 18 and 20 prevail even at this high temperature.

To analyse the high-temperature configurations we plot in figure 12 the thermal average of the one-electron spectrum of the non-magic 16 cluster and the cluster at the magic size $N = 20$, both at the temperature $T = 930\,\mathrm{K}$. For both the 16 cluster and the 20 cluster we observe a considerable broadening of the electronic levels due to the atomic motion, but an appreciable Fermi gap is still observed for both sizes. The broadening of the levels are seen to be several times $k_B T$. Similar level broadening is seen in experiment [22]. This is a consequence of the fact that only the total energy, and not the one-electron levels, are at a minimum in the ground-state structure of a cluster. Therefore there will be first-order variations in the position of a level as a function of coordinate fluctuations. In the harmonic approximation the size of coordinate fluctuations is proportional to $\sqrt{T}$, and therefore the leading term in the temperature variation of a one-electron level will also be proportional to $\sqrt{T}$, as opposed to the total energy, which is proportional to T. Even though the one-electron peak widths are large, the total energy only varies with thermal energies $\sim \sqrt{(3N-6)/2}\,k_B T$. For this reason it is still possible to see magic numbers at elevated temperature.

The clusters at $T = 930\,\mathrm{K}$ may be regarded as liquid in many respects, as we shall now show. The bulk melting point of copper is 1356 K, but it is well known that surfaces can introduce disorder or pre-melting at temperatures below the bulk melting temperature [24]. This phenomenon has also been studied using simulations based on the effective-medium theory [25]. The clusters are finite systems, and therefore we do not observe a phase transition in the usual thermodynamic sense, and there may even exist a temperature regime in which solid- and liquid-like phases coexist [26]. In the following we shall present some calculated finite-temperature values for quantities that give indications of the temperature at which the clusters can be regarded as melted: the eccentricity and the radial and angular correlation functions.

As a signature of the fluctuations in the overall shape of a cluster at a particular temperature we plot the average value of the smallest eccentricity ϵ_1 (8) in figure 13 for all cluster sizes at the same temperatures as in figure 11. We first observe that at $T = 460\,\mathrm{K}$ the spherical nature of the 13 cluster has been suppressed so that it falls more naturally on the Clemenger curve for the eccentricities. This is an indication that the shell energy is important at this temperature compared with the bulk-metal-like interactions that drove the 13 cluster spherical in the ground state. Most of the pronounced peaks in the curve have

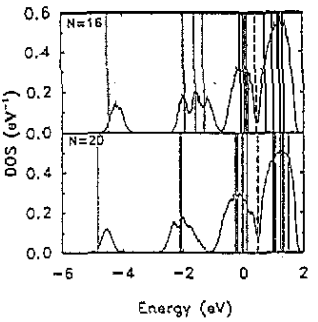

Figure 12. Temperature-averaged one-electron spectrum for the cluster $N = 20$ at $T = 930$ K. Broken curve: average E_F. Full vertical lines: energy levels from equilibrium structure, i.e. the one-electron spectrum at zero temperature. A large dip in the DOS at the Fermi level is still clearly seen even at this high temperature.

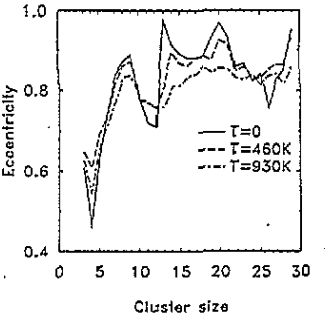

Figure 13. Average smallest eccentricity ϵ_1. Full curve: $T = 0$. Broken curve: $T = 460$ K. Chain curve: $T = 930$ K. The structure of the spectrum is smeared out at the higher temperatures; at the highest temperature the magic cluster $N = 20$ is no longer more spherical than its neighbours.

disappeared at $T = 930$ K, which is a sign that the clusters at this temperature sample a much larger region of phase space. However, as noted above, the clusters maintain appreciable Fermi gaps even at this temperature due to local Jahn–Teller distortions.

The detailed atomic structure is probed by the radial and angular correlation functions. In figure 14 the angular correlation function is shown for the 20 cluster for a range of temperatures. We observe that the pronounced peaks in the low-temperature spectra for the second, third and fourth nearest-neighbours disappear in a temperature regime around 230–460 K. This indicates a transition in the cluster to a more disordered 'phase' at this temperature.

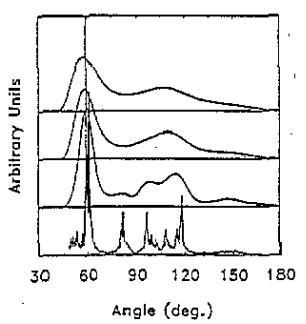

Figure 14. Angular correlation function at cluster size $N = 20$. A cutoff radius of 5.60 bohr was used, cf the previous figure. From bottom to top: $T = 0$ ground state, $T = 230$ K, $T = 460$ K and $T = 930$ K thermal averages. It is clearly indicated that the structure melts between the two temperatures $T = 230$ K and $T = 460$ K.

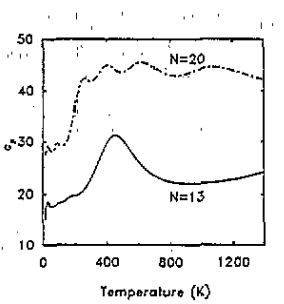

Figure 15. Heat capacity of Cu_{13} and Cu_{20} calculated [27] from energy distributions of Monte Carlo runs at different T. There is one well defined feature at $T \simeq 450$ K for Cu_{13}, indicating a finite-size smeared phase transition. The 20 cluster exhibits a complex behaviour with a deviation from the harmonic behaviour $c_p = (3N - 6)/2$ setting in below $T \simeq 200$ K.

On the basis of energy distributions for a whole set of Monte Carlo runs at different T it is possible [27] to give estimates of the classical density of states $W(E)$ such that

thermodynamic averages of functions of energy $f(E)$ can be calculated as

$$\langle f \rangle_T = \int \mathrm{d}E\, f(E)\, W(E)\, \mathrm{e}^{-E/k_B T}. \tag{9}$$

Using this method we have calculated the heat capacity c_p as a function of T for different cluster sizes. In figure 15 we show the results for $N = 13$ and $N = 20$. For Cu_{13} there is a clear indication of a smeared-out phase transition at $T \simeq 450\,\mathrm{K}$, whereas the picture for Cu_{20} is difficult to interpret. Studies of Lennard-Jones clusters [28] have indicated clear melting transitions for cluster sizes $N = 13$, 55 and 147, corresponding to closed Mackay icosahedra. Guided by the above-mentioned results for eccentricity and correlation functions as well as by observations of the configurations assumed by Cu_{13} at different temperatures it is possible to correlate the feature in the c_p curve with a transition from configurations with one well defined central atom to open configurations with no highly coordinated atoms.

The rise of c_p for Cu_{20} at very low T may be associated with soft shape oscillations or the possible existence of different isomers, as is found to be the case in recent theoretical studies of small Na and Si clusters [29]. The underlying mechanisms have not yet been sorted out in any detail. The results seem to indicate that cluster sizes corresponding to close-packed configurations are not necessarily representative of the thermodynamic properties of small clusters, and that further investigations of other sizes are necessary. This is also concluded in a recent paper [30] on small Be clusters. In this work, Be_{13} is seen to have a higher melting point than smaller Be clusters, probably as a consequence of the close-packed ground-state structure.

4. Conclusion

The effective-medium model with a tight-binding description of the shell energy has been shown to give a reliable description of the atomic structure of small Cu clusters. The calculated ground-state structures are in close agreement with experiment and other calculations and it reproduces the magic sizes observed experimentally. The coupling between the atomic and electronic degrees of freedom through a Jahn–Teller-like effect has been shown to have a number of important consequences. It is crucial for understanding the stability of the magic clusters at high temperatures and it is responsible for the strong even–odd oscillations which are experimentally observed. The atomic motion also plays a key role in the large broadening of the electronic levels observed in photoelectron spectroscopy. A phase transition of Cu_{13} at $T \simeq 450\,\mathrm{K}$ is indicated by various analyses of the Monte Carlo results, whereas clusters of other sizes show more complex behaviour.

Acknowledgments

Many stimulating discussions with J K Nørskov, M Manninen and P Stoltze are gratefully appreciated. The research has been supported by the Danish Research Councils through the Centre for Surface Reactivity.

References

[1] de Heer W A, Knight W D, Chou M Y and Cohen M L 1987 *Solid State Phys.* **40** 93
[2] Knight W D, Clemenger K, de Heer W A, Saunders W A, Chou M Y and Cohen M L 1984 *Phys. Rev. Lett.* **52** 2141
[3] Katakuse I, Ichihara I, Fujita Y, Matsuo T, Sakurai T and Matsuda H 1985 *Int. J. Mass Spectrom. Ion Proc.* **67** 229
[4] Clemenger K 1985 *Phys. Rev.* B **32** 1359
[5] Nilsson S G 1955 *K. Dan. Vidensk. Selsk. Mat. Fys. Medd.* **29** no. 16
Gustafson C, Lamm I L, Nilsson B and Nilsson S G 1967 *Ark. Fys.* **36** 613
[6] Ekardt W 1984 *Phys. Rev.* B **29** 158; 1985 *Surf. Sci.* **152/153** 180
[7] Ekardt W and Penzar Z 1988 *Phys. Rev.* B **38** 4273
[8] Wang Y, George T F, Lindsay D M and Beri A C 1987 *J. Chem. Phys.* **86** 3493
Lindsay D M, Wang Y and George T F 1987 *J. Chem. Phys.* **86** 3500
[9] Bonačić-Koutecký V, Fantucci P and Koutecký J 1990 *J. Chem. Phys.* **93** 3802
Bonačić-Koutecký V, Boustani I, Guest M and Koutecký J 1988 *J. Chem. Phys.* **89** 4861
[10] Martins J L, Buttet J and Car R 1985 *Phys. Rev.* B **31** 1804
[11] Manninen M 1986 *Phys. Rev.* B **34** 6886
Cocordan J A, Virkkunen R and Manninen M 1988 *Phys. Scri.* **38** 758
Rao B K, Khanna S N and Jena P 1987 *Phys. Rev.* B **36** 953
[12] Ballone P, Andreoni W, Car R and Parrinello M 1989 *Europhys. Lett.* **8** 73
Röthlisberger U and Andreoni W 1991 *J. Chem. Phys.* **94** 8129
[13] Garland D A and Lindsay D M 1984 *J. Chem. Phys.* **80** 4761
[14] Jacobsen K W, Nørskov J K and Puska M J 1987 *Phys. Rev.* B **35** 7423
Jacobsen K W 1988 *Comments Condens. Matter. Phys.* **14** 129
Chetty N, Stokbro K, Jacobsen K W and Nørskov J K 1992 *Phys. Rev.* B **46** 3798
[15] Christensen O B, Jacobsen K W, Nørskov J K and Manninen M 1991 *Phys. Rev. Lett.* **66** 2219
[16] Andersen O K and Jepsen O 1984 *Phys. Rev. Lett.* **53** 2571
Andersen O K, Jepsen O and Glötzel D 1985 *Highlights of Condensed-Matter Theory, LXXXIX Corso Soc. Italiana di Fisica, Bologna*
[17] Moruzzi V L, Janak J F and Williams A R 1978 *Calculated Electronic Properties of Metals* (Oxford: Pergamon)
[18] Binder K (ed) 1986 *Monte Carlo Methods in Statistical Physics (Topics in Current Physics 7)* (Berlin: Springer)
[19] Manninen M 1986 *Phys. Rev.* B **34** 6886
[20] Selby K, Vollmer M, Masui J, Kresin V, de Heer W A and Knight W D 1989 *Phys. Rev.* B **40** 5417
[21] Winter B J, Parks E K and Riley S J 1991 *J. Chem. Phys.* **94** 8618
[22] Pettiette C L, Yang S H, Craycraft M J, Conceicao J, Laaksonen R T, Cheshnovsy O and Smalley R E 1988 *J. Chem. Phys.* **88** 5377
[23] Rao B K and Jena P 1985 *Phys. Rev.* B **32** 2058
Bonačić-Koutecký V, Fantucci P and Koutecký J 1991 *Chem. Rev.* **91** 1035
[24] Frenken J W M, Maree P M J and van der Veen J F 1985 *Phys. Rev. Lett.* **54** 134
Pluis B, Denier van der Gon A W, Frenken J W M and van der Veen J F 1987 *Phys. Rev. Lett.* **59** 2678
[25] Stoltze P, Nørskov J K and Landman U 1988 *Phys. Rev. Lett.* **61** 440
[26] Berry R S, Jellinek J and Natanson G 1984 *Phys. Rev.* A **30** 919
[27] Ferrenberg A M and Swendsen R H 1989 *Phys. Rev. Lett.* **63** 1195
[28] Labastie P and Whetten R L 1990 *Phys. Rev. Lett.* **65** 1567
[29] Röthlisberger U and Andreoni W 1991 *Z. Phys.* D **20** 243
[30] Cai Z-X, Mahanti S D, Antonelli A, Khanna S N and Jena P 1992 *Phys. Rev.* B **46** 7841